Mechanical properties of additively manufactured composite materials with ultrasonically assembled reinforcement.

Thomas Llewellyn-Jones[a], Bruce Drinkwater[b], Richard Trask[a]
[a]ALM^{3}D, University of Bath, Claverton Down, Bath, United Kingdom, BA27AY
[b]Faculty of Engineering, University of Bristol, Bristol, BS81TR, UK

Abstract

This study demonstrates the use of ultrasonic manipulation to assemble short fibres into a desired orientation within a photocurable resin, in order to additively manufacture discontinuous fibre reinforced composite materials. An optimised postcure time of 5 minutes was determined, as well as a suitable fibre weight fraction of 0.05 g/ml, which would demonstrate anisotropy without significantly hindering either the alignment or printing processes. Samples were fabricated from neat resin, as well as fibre reinforced samples. All fibres were unidirectionally aligned, with one set of samples containing fibres aligned at 0° to the loading axis, and another set containing fibres aligned at 90° to the loading axis. These materials have subsequently been loaded in tension to failure, with the ultimate tensile strength and Youngs modulus subsequently calculated. A 103% increase in tensile strength and 64% increase in Youngs modulus was found with 0° fibres compared to the neat resin. An increase of 76% and 94% was observed between samples with fibres aligned along the loading axis and those with fibres aligned at 90° to the loading axis.

1 Introduction

Discontinuous fibre reinforced plastics (DFRPs) offer a number of significant advantages over continuous fibre reinforced plastics (CFRPs), most notably in terms of reducing manufacturing defects. The ability of DFRP's to conform to complex geometries without introducing process-related defects has made them an attractive alternative to CFRP's, which are prone to issues such as fibre wrinkling and in-plane waviness [1]. Currently DFRPs are typically reinforced with randomly aligned fibres in non-load bearing applications, such as using recycled-fibre mats to form lightweight automotive door panels. In order to maximise the reinforcing effect of the fibre inclusion, it is important to ensure that fibres are aligned along the load path of the component in question.

A number of techniques have been devised to align discontinuous fibres, both within additive manufacturing processes and preform fabrication. These techniques include magnetic field alignment [2, 3, 4], electric field alignment [5], nozzle-shearing [6] and ultrasonic manipulation[7, 8] within additive manufacturing processes, while DFRP preform fabrication is dominated by convergent fluid methods[9]. All of these have demonstrated their ability to generate anisotropic materials, with the HiPerDif process showing exceptionally high degrees of alignment [10]. These techniques are generally still constrained to simple, unidirectional or woven reinforcement structures. Field effect techniques, in combination with additive manufacturing processes, potentially offer significantly greater design freedom, both in component geometry and reinforcement structure.

In earlier work we have shown the potential for using acoustic manipulation in conjunction with a modified form of stereolithographic additive manufacturing to 3D print composite materials with tailored and complex reinforcement architectures [11]. Acoustophoresis is the process of using acoustic radiation forces to manipulate particles, either in isolation or as groups into assemblies. Ultrasonic manipulation been employed across a wide range of disciplines, including cell sorting in microfluidic vascules [12], formation of metamaterials for wave guiding [13], and particle size-sorting [14].

2 Materials and Methods

2.1 Sample Manufacturing

A commercial methacrylate photocurable resin was used as the host resin for suspending glass microfibres. The resin used is a commercially available photocurable methacrylate based system (Formlabs Clear Resin v1), designed for use with an SLA 3D printer, and is easily cured by any 405nm light source. Fibre alignment was produced using a disposable PMMA frame adhered to a glass substrate, with piezoceramic transducers used to generate a standing wavefield within a central cavity containing the resin/fibre mixture. The transducers are comprised of lead zirconate titanate (PZT) from a commercial supplier (Noliac Ceramics NCE51). The dimensions of the transducers are 35 mm x 2 mm x 0.975 mm, with conductive paint applied to the two faces across the 0.975mm dimension which act as the electrodes for the transducer. The innermost printing/assembly cavity in the PMMA frame has dimensions of 35 mm x 35 mm. Four outer cavities house the transducers, which are held in place pressed against the inner wall of the cavity by a small compression spring (Lee Spring CIM 040EG01S). These cavities are subsequently filled with water to act as a heatsink for the transducers. A schematic of the assembled ultrasonic device is shown in Figure 1. While the device enables the use of two pairs of opposing transducers, in this study only a single pair was required to generate the samples, as all samples are reinforced by unidirectionally aligned fibres. This is achieved by driving one opposing pair of transducers at the same frequency and voltage, resulting in a 1D standing wavefield produced by the counter-propagating waves. The acoustic radiation force manipulates the fibres towards the pressure nodal planes, and due to their aspect ratio a rotational force is also exerted, aligning the fibres along the planes. The resulting reinforcement structure consists of discrete bundles of aligned fibres separated by a half wavelength of the standing wavefield.

The manipulation device is placed on the print bed of a modified commercial FDM printer (SeeMeCNC Rostock Max v2). The key modification is the removal of the plastic extruder and hot end, which have been replaced by a switchable, focused 405 nm 50mW laser module. The laser is switched from a fan PWM supply on the printer control board via a relay, and so can be switched using standard G-code commands within a print file. The relay is required to switch the laser from the printer control board while using a separate 3.5 volt power supply to operate the laser module without damaging it. A digital relay was used to enable fast switching. This laser is used to selectively cure regions of photocurable resin within the ultrasonic device in a similar fashion to SLA 3D printing. A 1.5mm aperture was fixed on the end of the laser carriage to remove any light halo effects.

G-code toolpath files for this printer are generated using a similar process to that in conventional slicing of 3D models for FDM printers, with the use of an additional script to modify the files for the modified printing format. The model file used to create the tensile samples within this study was

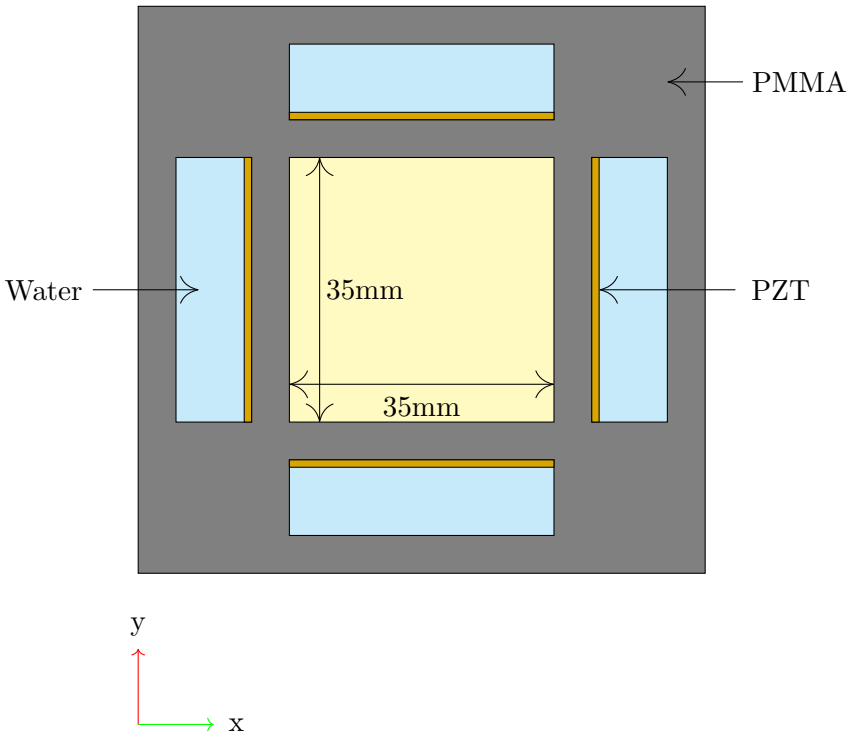

Figure 1: Schematic showing assembly of ultrasonic rig used for ultrasonic manipulation

constructed following the specifications from a tensile testing standard (ASTM D638), and scaled to fit within the internal printing cavity of the ultrasonic device. The model was generated as an STL (stereolithography) file. This was then converted into a G-code print file using a commercially available slicer (Cura v15.04). Following this the resulting G-code file was altered with a Matlab script which we had written specifically to generate a print file which would photocure the resin in the print cavity. As the current printing process only creates a single layer, only commands corresponding to the first layer of the G-code file are extracted. Hot end and print bed heating commands are removed from the preamble as these are not required for photocuring. All extrusion commands are removed for the same reason. In place of extrusion values, a command is inserted to active the PWM fan before any commands corresponding to extrusion and a command is inserted to disable the fan before any travel move. The relevant commands are 'M106' and 'M107' respectively. Once these alterations have been made, the print file is ready for use with the modified photocuring printer.

2.2 Sample Composition

In this study, the resulting effect of the assembled reinforcement on the mechanical properties of the material is determined through tensile testing of various compositions of the material.

Neat resin samples were tested as a material baseline, and the remaining samples contained unidirectionally aligned fibres either along the loading axis of the sample or at 90 degrees to the loading axis. In order to determine the mechanical properties of the printed material, a set of modified dogbone tensile test samples (from ASTM-D638-03) were printed with a number of fibre volume fractions and orientation angles (with respect to the loading angle). The test specimen was

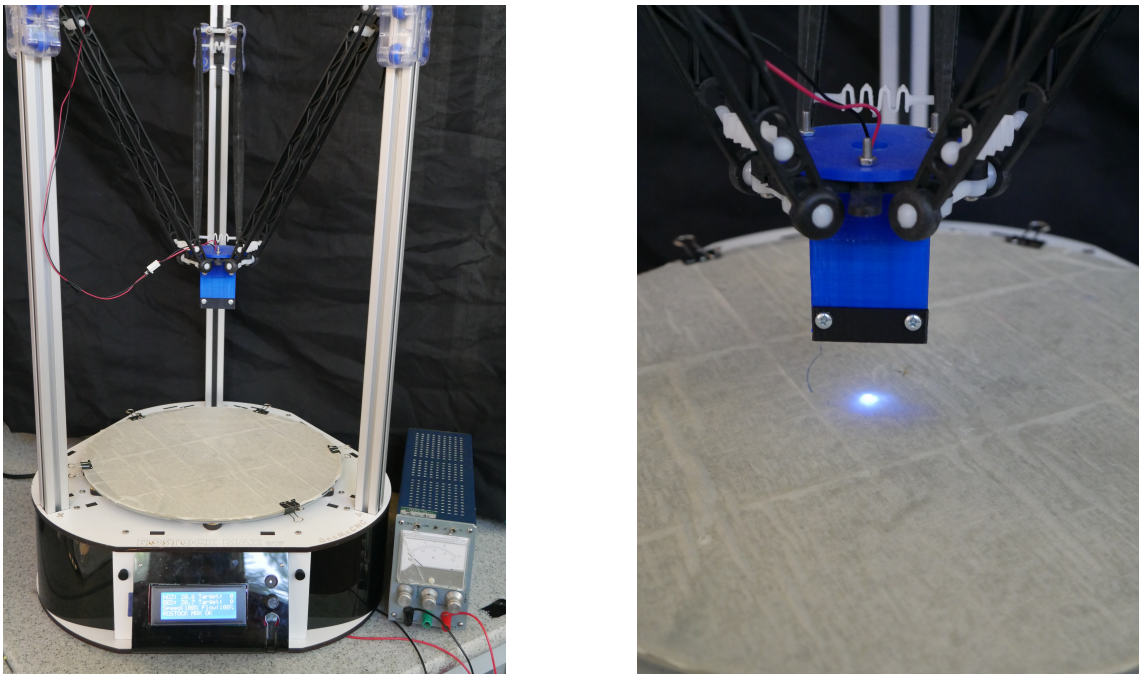

Figure 2: *Left* Modified Rostock Max v2 FFF printer. *Right* Demonstration of switched UV laser mounted on FFF printer carriage without aperture attached. The beam has a high intensity central region with a diameter of ∼0.75mm.

modified such that it would fit within the cavity of the acoustic manipulation device within the printer.

Three different compositions of reinforcement were fabricated for testing. A reference set of neat resin samples were produced as a baseline to measure improvements to mechanical properties with fibre reinforcement, and to determine the overall degree of anisotropy of samples with unidirectionally aligned reinforcement. Unidirectionally reinforced samples were also fabricated, with one set containing fibres aligned along the loading direction and the other set containing fibres aligned orthogonal to the loading axis.

2.3 Testing Protocol

Each of the manufactured samples were subsequently loaded to failure in tension, using a Shimadzu AGS-X electromechanical test frame with a 1kN load cell. The samples were loaded at a displacement rate of 0.10 mm min^{1}. Samples were held in place using screw-tightened grips with file teeth faces to prevent sample slippage. The resulting load-displacement data was used, along with the measured dimensions of each samples width, thickness and gauge length, to determine the yield strength and modulus of the material. Sample extension Δ was measured along the loading axis as a function of time. A strain to failure ϵ^* value was determined using this extension and the length L of the sample prior to loading:

$$\epsilon^* = \frac{\Delta}{L} \tag{1}$$

The failure strength σ^* was calculated using the maximum load F_{max} and the measured cross-

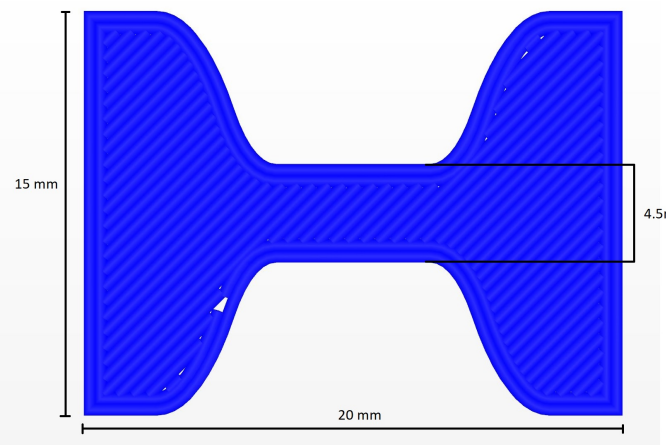

Figure 3: Schematic visualisation of the toolpath used to print the tensile samples used in this study.

sectional area A of the tensile sample:

$$\sigma^* = \frac{F_{max}}{A} \tag{2}$$

The resin is designed to be postcured following printing to achieve its optimum mechanical properties, and as such samples were tested with varying levels of postcure to determine the point of full curing. The samples were postcured in an enclosed reflective chamber housing a 36W 405nm lamp. This was determined by calculating the failure strength of samples with 2 minutes, 5 minutes and 10 minutes of postcuring, and finding the relationship between postcure time and these mechanical properties to find the level of postcuring after which no changes occurs. These results are shown in Figure 4.

From these results, it was calculated that 5 minutes of postcuring was sufficient to fully cure the resin to achieve the greatest mechanical properties. Larger variations in tensile strength are observed in the samples after 10 minutes of postcuring, which is likely a result of warping and internal microcracks formed from the sample being illuminated mostly from a single side of the sample.

In order to determine a useful fibre/matrix ratio to ensure anisotropy could be measured, samples were fabricated from neat resin, as well as with fibres weight fractions of 0.025 g/ml and 0.05 g/ml. The reinforcement in both cases was ultrasonically aligned along the loading axis, and all three sets of samples were tested in tension to failure. The resulting tensile strength with fibre volume fraction is shown in Figure 4.

The strength of modulus of samples with a 0.025 g/ml weight fraction of fibres showed no noticeable difference to the neat resin, whereas the samples with a weight fraction of 0.05 g/ml showed a 63% increase in strength and a 74% increase in stiffness. As a result, all reinforced samples for the remainder of this study use a weight fraction of 0.05 g/ml. While a larger volume fraction would also provide improve stiffness results, increasing fibre concentration within the resin generates a larger number of acoustic scatterers, as well as increases inter-fibre friction, thereby reducing the efficiency of the ultrasonic manipulation. The resulting reinforcement structure would exhibit less discrete bands of fibres, and lower degrees of fibre alignment, thereby producing a microstructure

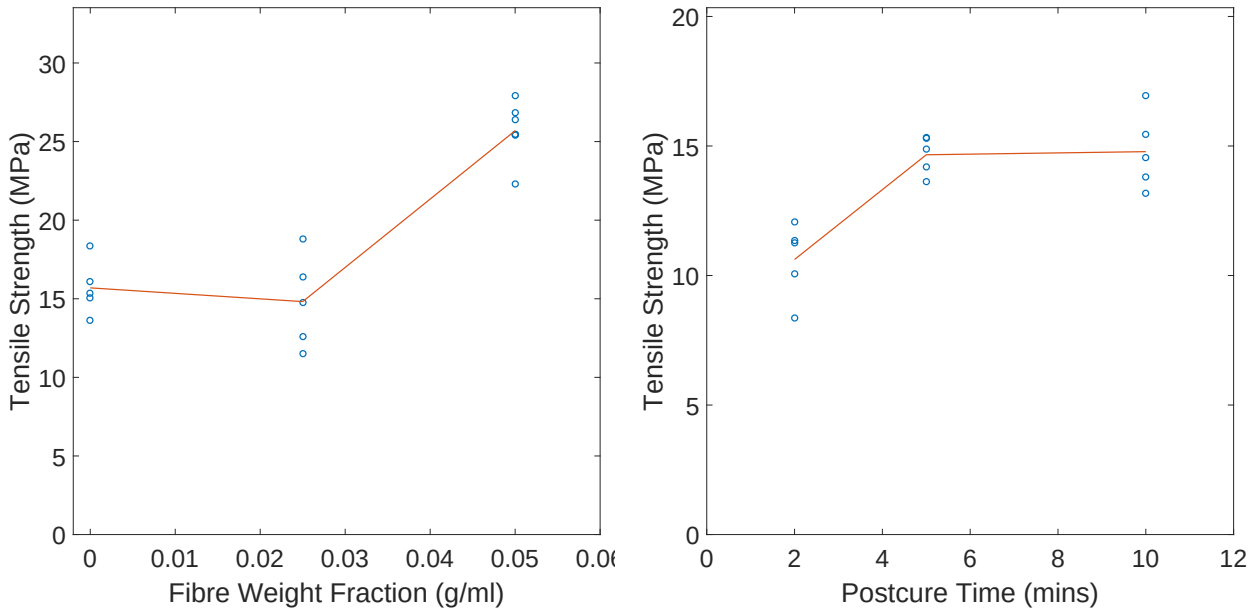

Figure 4: *Left:* Tensile strength vs postcuring time for neat resin samples. *Right:* Tensile strength vs fibre weight fraction, with fibres ultrasonically aligned along the loading axis.

more similar to a random fibre distribution with lower anisotropy. Including a larger fibre fraction would also interfere with the incident laser beam, and create greater inconsistencies in curing and lower printing resolution, due to refraction of the laser beam in the additional glass fibres.

3 Results and Discussions

Five samples of each reinforcement structure were fabricated and tested to failure under tension as described previously. All samples had been postcured for 5 minutes, and contained a fibre weight fraction of 0.05 g/ml. The results are shown in the form of stress vs strain plots, as shown in Figure 5.

The mean tensile strength and Youngs modulus for each sample set is shown in Table 1.

Sample Set	**Tensile Strength (MPa)**	**Youngs Modulus (MPa)**
Neat Resin	13.07±0.99	402±42
Fibres perpendicular to loading axis	15.06±2.33	341±53
Fibres along loading axis	26.55±0.94	661±52

Table 1: Mean tensile strength and modulus for each reinforcement structure.

Samples with reinforcing fibres aligned perpendicular to the loading axis have a slightly higher average tensile strength than the neat sample, and a significantly lower Youngs modulus, although the errors in these measured values will be large in part due to the non-uniformity in the cross sections of samples, with sample thickness varying from 0.4-0.8mm across their width. Samples with fibres aligned along the loading axis exhibited dramatically higher average tensile strength and modulus, with a 103% and 64% increase respectively as compared to the neat resin. As seen

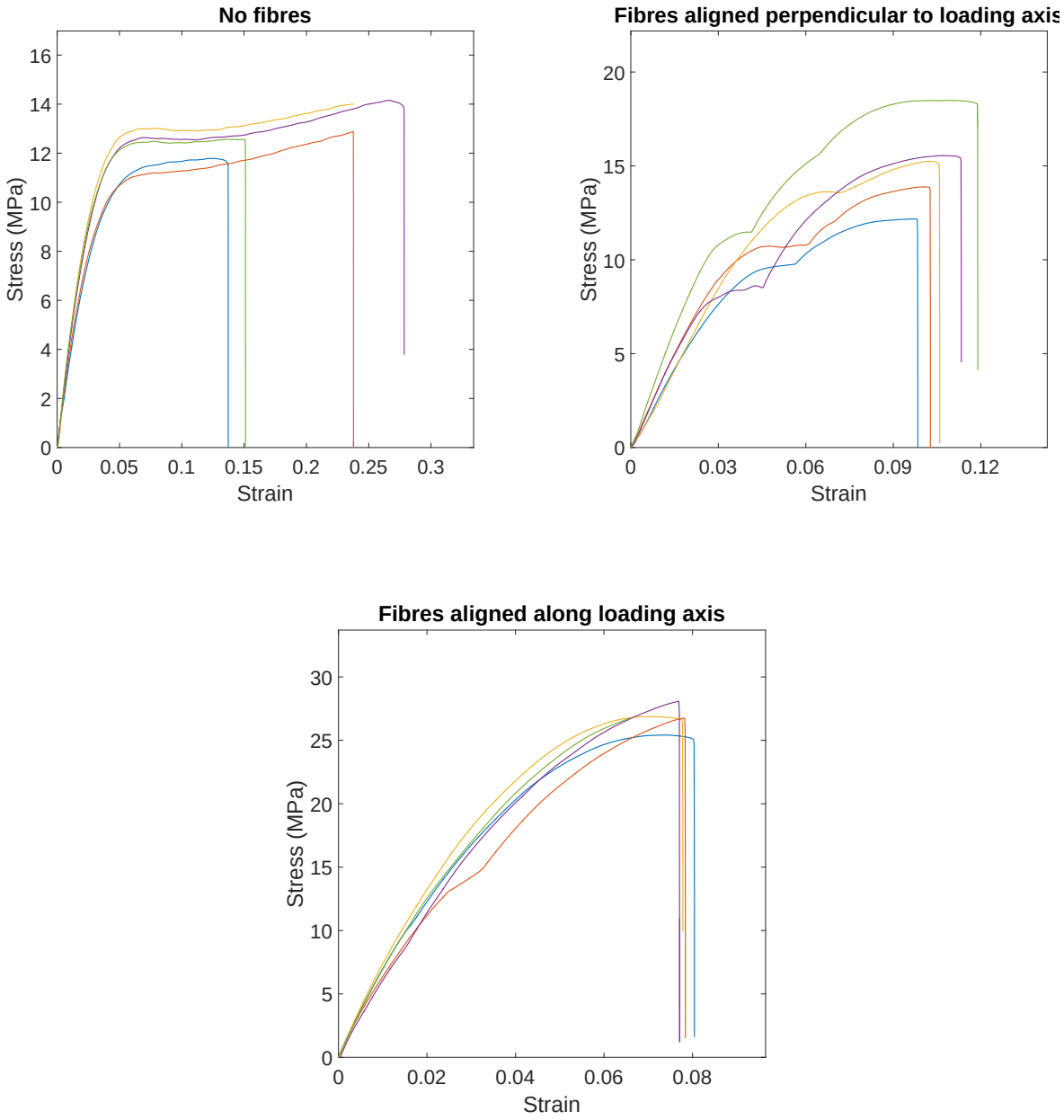

Figure 5: Stress-strain profiles of all samples tested in this study. *Top Left:* Neat resin samples with no fibrous reinforcement. *Top Right:* Samples with reinforcing fibres aligned at 90° to the loading axis. *Bottom Middle:* Samples with reinforcing fibres aligned along the loading axis.

in Figure 5, the neat resin underwent an extensive degree of plastic deformation before failure. The samples with 90° fibres showed some ductility, but noticeably less than the neat resin and with greater variability between samples. The load-axis aligned reinforced samples showed almost

no plastic deformation and reached far higher stresses before failure, indicating that the stiff and brittle glass fibres were being loaded by the matrix.

Samples with fibres aligned perpendicular to the loading axis showed a two-stage loading profile, with an increase in stiffness observed after a region of plastic deformation at a stress of 8-12 MPa. It is speculated that this occurs due to complex crack propagation paths which are formed due to misalignment between the desired reinforcement orientation and the final observed result. Any misalignment will be the result of imperfections in the ultrasonic rig, such as surface waviness of the laser cut frame and transducers not sitting perfectly flush to the cavity wall. This stress profile is the subject of ongoing investigation.

4 Conclusions

Discontinuous fibre reinforced composite materials were 3D printed with ultrasonically assembled microstructures, which were subsequently fractured under tensile load. From these tests the failure strength and Youngs modulus of the samples were determined. Using samples with fibres aligned along the loading axis, and samples with fibres aligned perpendicular to the loading axis, the large degree of anisotropy achievable by ultrasonically aligning fibres within an additively manufactured structure was demonstrated.

All the measured values are substantially lower than the manufacturer quoted properties for the fully cured material (65 MPa ultimate tensile strength and 2.6 GPa Youngs modulus), but due to the small size of the samples and unorthodox printing mechanism it would be unsurprising if small cracks, microbubbles and edge notches occurred frequently during manufacture.

Having loaded 5 samples to failure from each of the 3 sample compositions, a 76% and 94% increase were seen in the ultimate tensile strength and Youngs modulus, respectively, between samples with fibres aligned along the loading axis and those with fibres aligned at 90° to the loading axis.

5 Future Work

The primary focus for future work is to complete a case study which demonstrates a component which requires the localised stiffness increase provided by ultrasonically assembled reinforcement microstructures. A concept of particular interest is the idea of a thin membrane of neat resin with stiff reinforced ribs, replicating the structure of a bat wing. This would demonstrate that the use of ultrasonic assembly in conjunction with a modified SLA printing process is able to fabricate deployable, variable-stiffness structures with a single matrix and within a single print, which is currently not feasible with existing additive layer processes.

Other aspects of future work include forming complex microstructure reinforcements, repeatably printing consecutive layers, and increasing the fibre volume fraction that can be effectively aligned within a sample in order to maximise the mechanical properties of the final component.

Acknowledgements

This work was supported by the Engineering and Physical Sciences Research Council through the EPSRC Centre for Doctoral Training in Advanced Composites for Innovation and Science (grant number EP/G036772/1). The authors gratefully acknowledge the support of the UK Engineering

Physical Sciences Research Council (EPSRC) for funding Professor Richard S Trask's fellowship and research under EPSRC 'Engineering Fellowships for Growth', (grant number EP/M002489/1).

References

[1] James S. Lightfoot, Michael R. Wisnom, and Kevin Potter. Defects in woven preforms: Formation mechanisms and the effects of laminate design and layup protocol. *Composites Part A: Applied Science and Manufacturing*, 51:99–107, 2013.

[2] Joshua J. Martin, Brad E. Fiore, and Randall M. Erb *et al.* Designing bioinspired composite reinforcement architectures via 3D magnetic printing. *Nature Communications*, 6:8641, oct 2015.

[3] I. Kvien and K. Oksman. Orientation of cellulose nanowhiskers in polyvinyl alcohol, 2007.

[4] Tanittha Pullawan, Arthur N Wilkinson, and Stephen J Eichhorn. Influence of magnetic field alignment of cellulose whiskers on the mechanics of all-cellulose nanocomposites. *Biomacromolecules*, 13(8):2528–36, 2012.

[5] Vyakarnam and Murty N. A new process for aligning chopped fibers in composites. *Plastics Engineering*, 1997.

[6] W Zhong, F Li, Z Zhang, L Song, and Z Li. Short fiber reinforced composites for fused deposition modeling. *Materials Science and Engineering: A*, 301(2):125–130, mar 2001.

[7] M-S Scholz, B W Drinkwater, and R S Trask. Ultrasonic assembly of anisotropic short fibre reinforced composites. *Ultrasonics*, 54(4):1015–9, apr 2014.

[8] M. Saito and Y. Imanishi. Host-guest composites containing ultrasonically arranged particles. *Journal of Materials Science*, 35(10):2373–2377, 2000.

[9] Matthew Such, Carwyn Ward, and Kevin Potter. Aligned Discontinuous Fibre Composites: A Short History. *Journal of Multifunctional Composites*, 2(3), 2014.

[10] H. Yu, K.D. Potter, and M.R. Wisnom. A novel manufacturing method for aligned discontinuous fibre composites (High Performance-Discontinuous Fibre method). *Composites Part A: Applied Science and Manufacturing*, 65:175–185, oct 2014.

[11] Thomas M Llewellyn-Jones, Bruce W Drinkwater, and Richard S Trask. 3D printed components with ultrasonically arranged microscale structure. *Smart Materials and Structures*, 25(2):02LT01, feb 2016.

[12] A.L. Bernassau, P. Glynne-Jones, F. Gesellchen, M. Riehle, M. Hill, and D.R.S. Cumming. Controlling acoustic streaming in an ultrasonic heptagonal tweezers with application to cell manipulation. *Ultrasonics*, 54(1):268–274, 2014.

[13] Mihai Caleap and Bruce W Drinkwater. Acoustically trapped colloidal crystals that are reconfigurable in real time. *Proceedings of the National Academy of Sciences of the United States of America*, 111(17):6226–30, apr 2014.

[14] E.R. Dauson, I.J. Oppenheim, K.B. Gregory, and D.W. Greve. Microparticle separation using a PMMA channel at an oblique angle to a SAW field. In *2014 IEEE International Ultrasonics Symposium*, pages 1952–1955. IEEE, sep 2014.